Appl. Math. Mech. -Engl. Ed., **41**(10), 1447–1460 (2020)

APPLIED MATHEMATICS AND MECHANICS (ENGLISH EDITION)

https://doi.org/10.1007/s10483-020-2660-8

Shear-horizontal waves in periodic layered nanostructure with both nonlocal and interface effects*

Ru TIAN[1,2], Jinxi LIU[3,4,†], E. N. PAN[2], Yuesheng WANG[1]

1. Institute of Engineering Mechanics, Beijing Jiaotong University, Beijing 100044, China;
2. Department of Civil Engineering, University of Akron, Akron, OH 44325-3905, U. S. A.;
3. Department of Engineering Mechanics, Shijiazhuang Tiedao University, Shijiazhuang 050043, China;
4. Hebei Key Laboratory of Mechanics of Intelligent Materials and Structures, Shijiazhuang Tiedao University, Shijiazhuang 050043, China

(Received May 24, 2020 / Revised Jul. 10, 2020)

Abstract The propagation of shear-horizontal (SH) waves in the periodic layered nanocomposite is investigated by using both the nonlocal integral model and the nonlocal differential model with the interface effect. Based on the transfer matrix method and the Bloch theory, the band structures for SH waves with both vertical and oblique incidences to the structure are obtained. It is found that by choosing appropriate interface parameters, the dispersion curves predicted by the nonlocal differential model with the interface effect can be tuned to be the same as those based on the nonlocal integral model. Thus, by propagating the SH waves vertically and obliquely to the periodic layered nanostructure, we could invert, respectively, the interface mass density and the interface shear modulus, by matching the dispersion curves. Examples are further shown on how to determine the interface mass density and the interface shear modulus in theory.

Key words shear-horizontal (SH) wave, nonlocal theory, interface effect, nanostructure, integral model, differential model

Chinese Library Classification O347
2010 Mathematics Subject Classification 74J05

List of symbols

$c_{\rm sh}$,	bulk shear wave speed, m/s;		m;
e_{kl},	strain components;	$\overline{h}\,(=h_j/h)$,	dimensionless thickness;
f_l,	body force density in the l-direction	k,	wavenumber, m^{-1};
	$(l=x,\,y,\,z)$, $\mathrm{m/s}^2$;	k_x,	Bloch wavenumber in the
h,	thickness of the unit cell, m;		x-direction, m^{-1};
h_j,	thickness of the jth layer $(j=1,\,2)$,	kh/π,	dimensionless wavenumber;

* Citation: TIAN, R., LIU, J. X., PAN, E. N., and WANG, Y. S. Shear-horizontal waves in periodic layered nanostructure with both nonlocal and interface effects. *Applied Mathematics and Mechanics* (*English Edition*), **41**(10), 1447–1460 (2020) https://doi.org/10.1007/s10483-020-2660-8

† Corresponding author, E-mail: liujx02@hotmail.com

Project supported by the National Natural Science Foundation of China (Nos. 11472182 and 11272222) and the China Scholarship Council (No. 201907090051)

l_1,	material intrinsic length which represents the size of the interface mass density, m;		adjacent unit cells;
		u_l,	displacement in the l-direction, m;
l_2,	material intrinsic length which represents the size of the interface shear modulus, m;	$\boldsymbol{V}$,	state vector;
		$\boldsymbol{x}, \boldsymbol{x}'$,	position vectors;
l_1/h,	dimensionless material intrinsic length which represents the size of the interface mass density;	x, y, z,	variables in the rectangular coordinate system, m;
		$\alpha(\lvert\boldsymbol{x}' - \boldsymbol{x}\rvert)$,	influence function;
l_2/h,	dimensionless material intrinsic length which represents the size of the interface shear modulus;	β,	dimensionless wavenumber in the y-direction;
		ε,	internal characteristic length, m;
$R\,(=\varepsilon/h)$,	dimensionless internal characteristic length;	ξ, η,	dimensionless variables in the rectangular coordinate system;
		θ,	incidence angle, °;
$R_{\rm d}\,(=\varepsilon_{\rm d}/h)$,	dimensionless internal characteristic length in the nonlocal differential model;	λ, μ,	Lamé constants, $\mathrm{N/m^2}$;
		ρ,	mass density, $\mathrm{kg/m^3}$;
		$\rho_{\rm s}$,	interface mass density, $\mathrm{kg/m^2}$;
$R_{\rm i}\,(=\varepsilon_{\rm i}/h)$,	dimensionless internal characteristic length in the nonlocal integral model;	σ_{kl},	local stress components, $\mathrm{N/m^2}$;
		τ_{kl},	nonlocal stress components, $\mathrm{N/m^2}$;
		$\tau^{\rm s}_{zy}$,	interface stress components, N/m;
$\boldsymbol{R}$,	transfer matrix of the sub-layer;	ω,	angular frequency, rad/s;
t,	time, s;	ϖ,	dimensionless angular frequency;
$\boldsymbol{T}$,	transfer matrix between the two	Ω,	dimensionless frequency.

1 Introduction

As new functional materials, periodic layered composites can suppress the propagation of elastic waves within a certain frequency range[1–4]. The band-gap properties of periodic structures have broad applications in designing acoustic devices such as filters[5], transducers[6], acoustic lens[7], and waveguides[8]. Since these applications of periodic composites are closely related to the propagation properties of elastic waves, waves in the periodic structure need to be investigated.

Nanomaterials have excellent material properties, and they are easily tuned to meet the requirements of the relevant micro devices[9–11]. Based on the first-principle method at the atomistic level and the classical elastic wave equation at the continuum level, Ramprasad and Shi[12] compared the acoustic dispersion curves of a multilayer nano-heterostructure made of alternating HfO_2 and ZrO_2 layers, and found that the wave propagation properties in nanoscale were different from those in macroscale. When the structure dimension is reduced to the nanometer scale, the interface effect dominates. As such, various theories have been proposed to investigate the material behaviors in nanoscale as relative to those in macroscale[13]. Those include the couple stress theory[14–15], the micropolar theory[16], the strain gradient theory[17], the nonlocal theory[18–19], the nonlocal strain gradient theory[20–21], and the surface/interface theory[22–23].

By using the nonlocal theory of integral form (or simply called the nonlocal integral model), Chen and Wang[24] studied the shear wave which propagates normally in the one-dimensional nanoscale HfO_2-ZrO_2 phononic crystal and found that the first two bands of the dispersion curves were identical to those based on the first-principle method. In other words, the proper nonlocal theory could be used to describe the dispersion behaviors of the nanoscale multilayer structure. The concept of localization factor was introduced by Chen et al.[25] to describe the dispersion relations of the elastic waves propagating both normally and obliquely in the periodic nanostructure. Chen et al.[26] obtained analytical solutions for the time-harmonic waves in three-dimensional magneto-electro-elastic multilayered plates by using the nonlocal theory of differential form (or simply called the nonlocal differential model). The dispersion characteristics of elastic waves propagating in a monolayer piezoelectric nanoplate

were investigated by Zhang et al.[27] via the extended nonlocal differential model combining further with the surface piezoelectricity. Based on the surface/interface elasticity theory, the shear-horizontal (SH) waves in a transversely isotropic magneto-electro-elastic nanoplate[28] and the dispersion characteristics of SH waves in two dissimilar nanolayers[29] were studied. Zhu et al.[30] obtained the dispersion curves of layered nanostructures by using the Stroh formalism and the dual variable and position method. So far, however, the difference between the nonlocal integral model and the nonlocal differential model, with and without the surface/interface effect has not been fully explored, particularly as related to the dispersion curves predicted by different models. This motivates the present study.

Thus, in this paper, the SH waves which propagate vertically and obliquely in the periodic layered nanostructure are studied by using both the nonlocal integral and differential models with and without the interface effect. The band structures for such SH waves are obtained based on the transfer matrix method and the Bloch theory. This paper is arranged as follows. In Section 2, we describe the problem to be solved through the basic equations and interface conditions. In Section 3, the dispersion equations in the periodic layered nanostructure based on the nonlocal model with the interface effect are derived via the transfer matrix method and the Bloch theory. In Section 4, the effects of the nonlocal integral model, the nonlocal differential model with interface parameters (interface mass density and shear modulus) on the band structures (also dispersion curves) are analyzed when the SH waves are vertically and obliquely incident to the periodic structure. Conclusions are drawn in Section 5.

2 Problem description and basic equations

As shown in Fig. 1, the SH waves propagate to the isotropic periodic layered nanostructure with an incidence angle θ. For this case, the only nonzero displacement component is u_z as a function of x and y. The periodic layered nanostructure is composed of materials 1 and 2 alternatively, with thicknesses h_1 and h_2, respectively. As such, the thickness of the unit cell is $h = h_1 + h_2$.

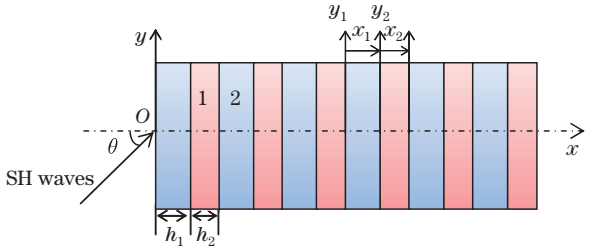

Fig. 1 SH waves propagation in a periodic layered nanostructure (color online)

For a homogeneous and isotropic elastic solid, the basic equations with consideration of the nonlocal theory can be expressed as[19]

$$\tau_{kl,l} + \rho\left(f_l - \ddot{u}_l\right) = 0, \tag{1}$$

$$\tau_{kl}\left(\boldsymbol{x}\right) = \int_v \alpha\left(|\boldsymbol{x}' - \boldsymbol{x}|\right)\sigma_{kl}\left(\boldsymbol{x}'\right)\mathrm{d}v\left(\boldsymbol{x}'\right), \tag{2}$$

$$\sigma_{kl}\left(\boldsymbol{x}'\right) = \lambda e_{jj}\left(\boldsymbol{x}'\right)\delta_{kl} + 2\mu e_{kl}\left(\boldsymbol{x}'\right), \tag{3}$$

$$e_{kl}\left(\boldsymbol{x}'\right) = \frac{1}{2}\Big(\frac{\partial u_k\left(\boldsymbol{x}'\right)}{\partial x'_l} + \frac{\partial u_l\left(\boldsymbol{x}'\right)}{\partial x'_k}\Big), \tag{4}$$

where δ_{kl} is the Kronecker delta function; τ_{kl}, ρ, f_l, and u_l are the nonlocal stress, the mass density, the body force density and displacement, respectively; a dot over u denotes time derivative; $\boldsymbol{x}$ and $\boldsymbol{x}'$ are the position vectors, and σ_{kl} are the local stress components related to

the strain components e_{kl} and Lamé constants λ and μ; $\alpha(|\boldsymbol{x}'-\boldsymbol{x}|)$ is the influence function. For the two-dimensional problem considered in this paper, we choose the following simple form[31]:

$$\alpha\left(|\boldsymbol{x}'-\boldsymbol{x}|,\varepsilon\right)=\frac{1}{2\varepsilon}\mathrm{e}^{-|x'-x|/\varepsilon}\delta\left(|y'-y|\right), \tag{5}$$

where δ is the Dirac delta function, and ε is the internal characteristic length. With the help of the differential operator, the constitutive equation of integral form, Eq. (2), can be approximated by the following differential form:

$$\left(1-\varepsilon^2\nabla^2\right)\tau_{kl}=\sigma_{kl}, \tag{6}$$

where ∇^2 is the two-dimensional Laplace operator. Substituting Eqs. (3), (4), and (6) into Eq. (1), the differential wave equation without the body force can be expressed as

$$(\lambda+\mu)\,u_{k,lk}+\mu u_{l,kk}=\left(1-\varepsilon^2\nabla^2\right)\rho\ddot{u}_l. \tag{7}$$

For this anti-plane problem, Eq. (7) can be reduced to the following simple form:

$$c_{\mathrm{sh}}^2\nabla^2 u_z=\left(1-\varepsilon^2\nabla^2\right)\ddot{u}_z, \tag{8}$$

where c_{sh} is the bulk shear wave speed defined as $c_{\mathrm{sh}}^2=\mu/\rho$. By introducing the dimensionless local coordinates $\xi=x/h$ and $\eta=y/h\,(\xi\in[0,\overline{h}],\eta\in(-\infty,+\infty))$ with $\overline{h}=h_j/h\,(j=1,2)$, the general solution to Eq. (8) can be expressed as

$$u_z=\left(A\mathrm{e}^{-\mathrm{i}q\xi}+B\mathrm{e}^{\mathrm{i}q\xi}\right)\mathrm{e}^{\mathrm{i}(\beta\eta-\omega t)}, \tag{9}$$

where A and B are undetermined constants, $\mathrm{i}^2=-1$, $\beta\ (=kh\sin\theta)$ is the dimensionless wavenumber in the y-direction, ω is the angular frequency, t is the time, and

$$q=\sqrt{\varpi^2/\left(1-R^2\varpi^2\right)-\beta^2} \tag{10}$$

with $\varpi=\omega h/c_{\mathrm{sh}}$ being the dimensionless angular frequency and $R=\varepsilon/h$ being the dimensionless internal characteristic length (i.e., the ratio of the internal to external characteristic lengths). From Eqs. (3), (4), and (6), we obtain the nonlocal stress in terms of the differential form as

$$\tau_{zx}^{\mathrm{d}}=\frac{\mathrm{i}\rho c_{\mathrm{sh}}^2 q\left(-A\mathrm{e}^{-\mathrm{i}q\xi}+B\mathrm{e}^{\mathrm{i}q\xi}\right)}{1+R^2q^2+R^2\beta^2}, \tag{11}$$

where the superscript d stands for the differential form. On the other hand, from Eqs. (2)–(5), the nonlocal stress based on the integral form can be expressed as

$$\begin{aligned}\tau_{zx}^{\mathrm{I}}&=\int_0^{\overline{h}}\frac{1}{2R}\mathrm{e}^{-\frac{|\xi'-\xi|}{R}}\mu\frac{\partial u_z}{\partial\xi'}\mathrm{d}\xi'\\&=\frac{-\mathrm{i}\rho c_{\mathrm{sh}}^2 q}{2}\Big(\Big(\frac{\mathrm{e}^{-\mathrm{i}q\xi}-\mathrm{e}^{-\xi/R}}{1-\mathrm{i}Rq}-\frac{\mathrm{e}^{-\mathrm{i}q\overline{h}}\mathrm{e}^{\left(\xi-\overline{h}\right)/R}-\mathrm{e}^{-\mathrm{i}q\xi}}{1+\mathrm{i}Rq}\Big)A\\&\quad-\Big(\frac{\mathrm{e}^{\mathrm{i}q\xi}-\mathrm{e}^{-\xi_j/R_j}}{1+\mathrm{i}Rq}-\frac{\mathrm{e}^{\mathrm{i}q\overline{h}}\mathrm{e}^{\left(\xi-\overline{h}\right)/R}-\mathrm{e}^{\mathrm{i}q\xi}}{1-\mathrm{i}Rq}\Big)B\Big),\end{aligned} \tag{12}$$

where the superscript I stands for the integral form.

To solve the problem, we also need the interface conditions. Based on the interface theory, the interface conditions between the two layers can be expressed as[23]

$$\begin{cases}u_{z\mathrm{R}}=u_{z\mathrm{L}},\\ \tau_{zx\mathrm{R}}-\tau_{zx\mathrm{L}}=\rho_{\mathrm{s}}\ddot{u}_3-\tau_{zy,y}^{\mathrm{s}},\end{cases} \tag{13}$$

where subscripts L and R denote the left and right sides of the interface, and $\rho_{\rm s}$ and $\tau^{\rm s}_{zy}$ are, respectively, the interface mass density and the interface stress. Notice that the units of the interface parameters (with superscript or subscript s) are different from those in the bulk material. In this paper we consider the following three cases: the nonlocal stress in the integral form without the interface effect (i.e., $\rho_{\rm s} = \tau^{\rm s}_{zy} = 0$ in Eq. (13)), the nonlocal stress in the differential form without the interface effect (i.e., $\rho_{\rm s} = \tau^{\rm s}_{zy} = 0$ in Eq. (13)), and the nonlocal stress in the differential form combined further with the interface effect (i.e., the general case of Eq. (13)).

For the nonlocal case in the differential form with the interface effect, we find that the nonlocal interface stress can be expressed as (from Eq. (6))

$$\tau^{\rm s}_{zy} = \sigma^{\rm s}_{zy}/(1 + R^2q^2 + R^2\beta^2), \tag{14}$$

where R and q take the values on the interface, and the local interface stress can be obtained by the following constitutive equation:

$$\sigma^{\rm s}_{zy} = \mu_{\rm s} u_{z,y}. \tag{15}$$

3 The transfer matrix and dispersion relation

The state vector is defined as $\boldsymbol{V} = (u_z, \tau_{zx})^{\rm T}$. Then, its values on the left and right sides of each sub-layer in the kth unit cell can be expressed as

$$\begin{cases} \boldsymbol{V}^k_{\rm L} = (u_z, \tau_{zx})^{\rm T}_{\xi=0} = \boldsymbol{M}(A, B)^{\rm T}, \\ \boldsymbol{V}^k_{\rm R} = (u_z, \tau_{zx})^{\rm T}_{\xi=\overline{h}} = \boldsymbol{N}(A, B)^{\rm T}, \end{cases} \tag{16}$$

where $\boldsymbol{M}$ and $\boldsymbol{N}$ are 2×2 matrices. Their elements can be obtained from Eqs. (9), (11) or (12) as listed in Appendix A. Eliminating the coefficients in Eq. (16), we then obtain the relation between the state vectors on the left and right sides of the sub-layer as

$$\boldsymbol{V}^k_{\rm R} = \boldsymbol{N}\boldsymbol{M}^{-1}\boldsymbol{V}^k_{\rm L} \triangleq \boldsymbol{R}\boldsymbol{V}^k_{\rm L}, \tag{17}$$

where $\boldsymbol{R} = \boldsymbol{N}\boldsymbol{M}^{-1}$ is the transfer matrix of the sub-layer.

The interface condition (see Eq. (13)) indicates that, on the interface between the sub-layer of the kth unit cell, the displacement is continuous whilst the traction is not. The general interface relations are

$$\begin{cases} u^k_{z2{\rm L}} = u^k_{z1{\rm R}}, \\ \tau^k_{zx2{\rm L}} - \tau^k_{zx1{\rm R}} = \rho_{\rm s}\ddot{u}_z - \tau^{\rm s}_{zy,y}, \end{cases} \tag{18}$$

where the subscripts 1 and 2 stand for the 1st and 2nd sub-layers, respectively. Combining Eqs. (14) and (16), we can rewrite Eq. (18) as

$$\boldsymbol{V}^k_{2{\rm L}} - \boldsymbol{V}^k_{1{\rm R}} = \boldsymbol{P}(A_2, B_2)^{\rm T}_k = \boldsymbol{P}\boldsymbol{M}_2^{-1}\boldsymbol{V}^k_{2{\rm L}}, \tag{19}$$

where $\boldsymbol{P}$ is a 2×2 matrix with its elements listed in Appendix A. Then, by combining Eqs. (17) and (19), we can finally obtain the relation of the state vectors between the left of 1st sub-layer and the right of 2nd sub-layer in the kth unit cell after passing the general interface as described by Eq. (13),

$$\boldsymbol{V}^k_{2{\rm R}} = \boldsymbol{R}_2(\boldsymbol{I} - \boldsymbol{P}\boldsymbol{M}_2^{-1})^{-1}\boldsymbol{R}_1\boldsymbol{V}^k_{1{\rm L}}, \tag{20}$$

where $\boldsymbol{I}$ is the 2×2 unit matrix. Similarly, we consider the 2nd sub-layer's right side of the $(k-1)$th unit cell and the 1st sub-layer's left side of the kth unit cell, by using the interface condition (13) and the relation (17). This gives us

$$\boldsymbol{V}_{2\mathrm{R}}^{k-1} = (\boldsymbol{I} - \boldsymbol{P}\boldsymbol{M}_1^{-1})\boldsymbol{V}_{1\mathrm{L}}^{k}. \tag{21}$$

From Eqs. (20) and (21), we finally derive

$$\boldsymbol{V}_{2\mathrm{R}}^{k} = \boldsymbol{R}_2(\boldsymbol{I} - \boldsymbol{P}\boldsymbol{M}_2^{-1})^{-1}\boldsymbol{R}_1(\boldsymbol{I} - \boldsymbol{P}\boldsymbol{M}_1^{-1})^{-1}\boldsymbol{V}_{2\mathrm{R}}^{k-1} \triangleq \boldsymbol{T}_k\boldsymbol{V}_{2\mathrm{R}}^{k-1}, \tag{22}$$

where $\boldsymbol{T}_k = \boldsymbol{R}_2(\boldsymbol{I} - \boldsymbol{P}\boldsymbol{M}_2^{-1})^{-1}\boldsymbol{R}_1(\boldsymbol{I} - \boldsymbol{P}\boldsymbol{M}_1^{-1})^{-1}$ is the 2×2 transfer matrix between the two adjacent unit cells. Considering the periodicity of the layered structure, for all $k = 1, 2, \cdots$, the matrix $\boldsymbol{T}_k$ is the same. Therefore, it can be denoted as $\boldsymbol{T}$ without the subscript k.

Now through the Bloch theorem[32], we have

$$\boldsymbol{V}_{2\mathrm{R}}^{k} = \mathrm{e}^{\mathrm{i}k_x h}\boldsymbol{V}_{2\mathrm{R}}^{k-1}, \tag{23}$$

where k_x is the Bloch wave number in the x-direction. Combining Eqs. (22) and (23), the following eigenvalue equation can be obtained:

$$\det\left(\boldsymbol{T} - \mathrm{e}^{\mathrm{i}k_x h}\boldsymbol{I}\right) = 0. \tag{24}$$

Therefore, for the given frequency ω, k_x can be solved from Eq. (24). If the solved k_x is a real number, then it means that the waves at the given frequency can propagate in the periodic layered structure. If k_x is an imaginary number, on the other hand, then the wave at the given frequency cannot propagate in the structure.

It is further noticed that when $\mu_{\mathrm{s}} = \rho_{\mathrm{s}} = 0$ and considering the nonlocal integral model, the problem is then reduced to the layered nanostructure of Ref. [24].

4 Numerical results and discussion

The solutions derived above are now used to calculate the dispersion relation. In order to compare our results with those obtained by the first-principle method, the materials of layers 1 and 2 are selected as HfO_2 and ZrO_2, respectively. The mass densities and bulk shear wave speeds of HfO_2 and ZrO_2 are $\rho_1 = 10\,873$ kg/m^3, $\rho_2 = 6\,488$ kg/m^3, $c_{\mathrm{sh1}} = 779$ m/s, and $c_{\mathrm{sh2}} = 1\,030$ m/s. It should be noted that while the surface material parameters should be determined from the detailed atomistic calculations or the experimental methods[27], such values for the interface between HfO_2 and ZrO_2 have been unavailable in the literature so far. By comparing the surface equation in the absence of residual stress with the approximate boundary conditions obtained by Mindlin[33] and utilized by Tiersten[34], Gurtin and Murdoch[23] concluded that the surface moduli are merely scaled versions of their bulk counterparts. Therefore, in the following computation, the interface material constants are assumed to be proportional to the bulk ones as

$$\rho_{\mathrm{s}} = l_1\rho_2, \quad \mu_{\mathrm{s}} = l_2\mu_2. \tag{25}$$

It is noted that since the units of the interface mass density and the interface shear modulus have different units as compared with their corresponding bulk parameters, the proportional coefficients l_1 and l_2 have the unit of length, denoting as the material intrinsic length. These intrinsic lengths represent, respectively, the sizes of the interface mass density and the interface shear modulus. In the part of numerical calculation, we use both the positive and negative interface material constants. This is due to the fact that the interface cannot solely exist without the bulk material and that the interface material constants can be positive or negative

depending on the material type and crystal orientation[35–36]. In the following calculation, the thicknesses of layers 1 and 2 are assumed as $h_1 = h_2 = 0.5h$. The internal characteristic lengths in each layer and on the interface are assumed to be the same, namely, $\varepsilon_1 = \varepsilon_2 = \varepsilon_s = \varepsilon$ or $R_1 = R_2 = R_s = R$. For convenience, the dimensionless frequency $\Omega = \omega h/(2\pi c_{sh1}) = \varpi_1/(2\pi)$, the dimensionless wavenumber kh/π, and the dimensionless material intrinsic length $l_j/h\,(j = 1, 2)$ are also introduced.

4.1 Vertical incidence

We first study the SH waves propagating vertically to the periodic layered nanostructure (i.e., $\theta = 0$ in Fig. 1). In this case, the nonzero displacement u_z is a function of x and t only, and therefore the only nonzero stress component is σ_{zx}. This means that only the interface mass density ρ_s will be involved in the interface material parameter. Figure 2 shows the band structures in terms of the dimensionless frequency Ω and the dimensionless wavenumber kh/π. From Fig. 2(a) for the nonlocal model without the interface effect ($l_1/h = 0$), we can see that the internal characteristic length has a great effect on the dispersion curve. At a given wavenumber, the nonlocal differential model (denoted by the subscript d to R as R_d) decreases the frequency and the nonlocal integral model (denoted by the subscript i to R as R_i) increases the frequency in the low frequency region ($\Omega < 1$). Figure 2(b) plots the influence of the local model ($R = 0$) with the interface effect on the dispersion curves. It is observed from Fig. 2(b) that, at a given wavenumber, a positive interface mass density decreases the frequency whereas a negative one increases the frequency. The interesting features in Figs. 2(a) and 2(b) indicate that by adjusting the negative interface mass density l_1, the dispersion curves obtained by the nonlocal differential model can be tuned to be the same as those from the nonlocal integral model (when $R_i = R_d$). This is shown in Fig. 2(c) when $R\,(= R_i = R_d) = 0.05$ with an adjusted value l_1. Such a striking feature in Fig. 2(c) demonstrates further that the interface parameters could be predicted or inverted by matching the band structures based on both the nonlocal integral and differential models.

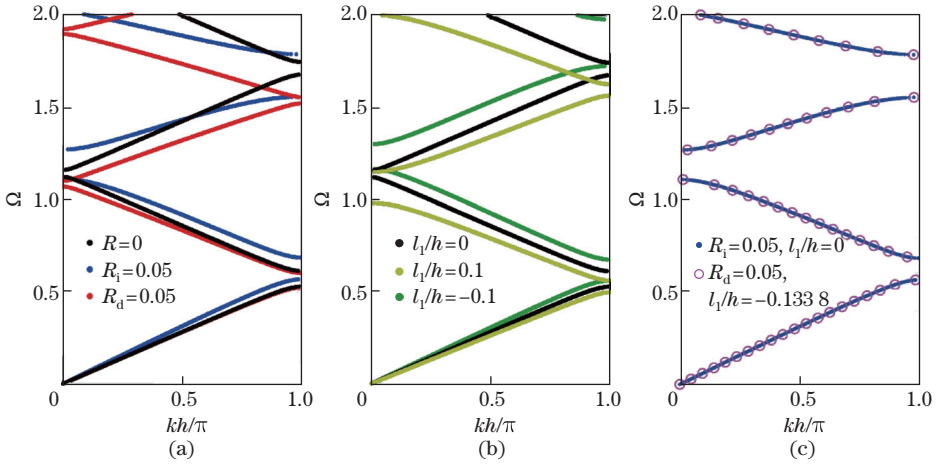

Fig. 2 Dispersion curves for the SH waves vertically incident to the HfO_2-ZrO_2 periodic layered nanostructure, (a) the nonlocal model without the interface effect ($l_1/h = 0$), (b) the local model ($R = 0$) with the interface effect, and (c) the model with combined effects (color online)

The band structures based on the nonlocal integral model, the nonlocal differential model, and the nonlocal differential model with the interface effect for $R\,(= R_i = R_d) = 0.1$ are shown in Fig. 3. It is observed from Fig. 3(a) that, the cut-off frequency is the same based on both the nonlocal differential and integral models. Figure 3(b) shows that, when the interface parameter is $l_1/h = -0.259\,9$, the band structures obtained by the nonlocal differential model

are almost the same as those based on the nonlocal integral model when $R(=R_{\mathrm{i}}=R_{\mathrm{d}})=0.1$. Furthermore, the cut-off frequency is not affected by the interface parameter when $R(=R_{\mathrm{i}}=R_{\mathrm{d}})=0.1$. These interesting features suggest that there exist some intrinsic relations between the internal characteristic length and the interface parameter, which will be investigated later. Additionally, near $\Omega=1.5$ and 2, the bands are very dense and almost flat, which show a strong wave localization phenomenon in these frequency ranges.

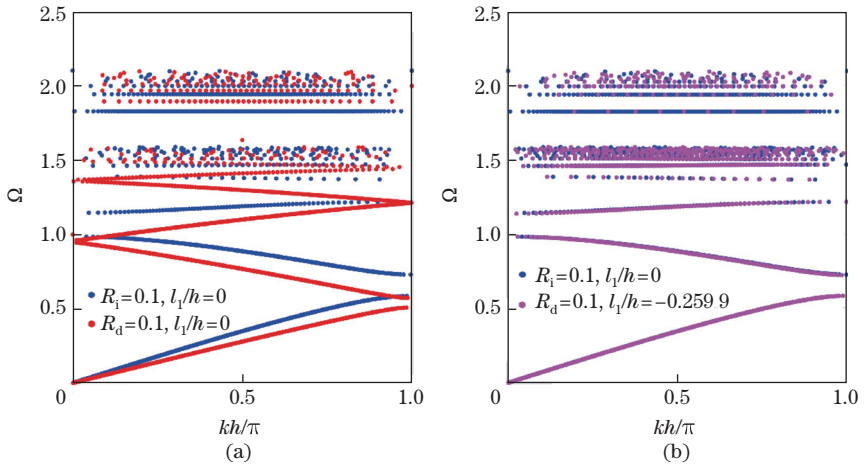

Fig. 3 Dispersion curves for the SH waves vertically incident to the HfO_2-ZrO_2 periodic layered nanostructure, (a) the nonlocal model without the interface effect ($l_1/h=0$) and (b) the model with combined effects (color online)

We point out that the nonlocal differential model combined with the interface effect could be very accurate towards wave modeling in nanoscale. As an example, we present in Fig. 4 the comparison of the first two SH waves bands in the HfO_2-ZrO_2 periodic layered nanostructure, based on the first-principle by Ramprasad and Shi[12] and the present approach. The parameters used are $h_1=h_2=0.501\,5$ nm (or $R=0.18$), and the waves are propagating vertically in the structure. An angular frequency $\omega=1\ 000$ GHz here corresponds to a dimensionless frequency $\Omega=0.210\ 4$ in Fig. 3. It is observed from Fig. 4 that the band structures predicted by the nonlocal integral model and the nonlocal differential model with the interface density parameter $l_1/h=-0.404\ 3$ are identical to those based on the first-principle method (see Ref. [12]). This excellent agreement opens a possible new path to inverting the interface mass

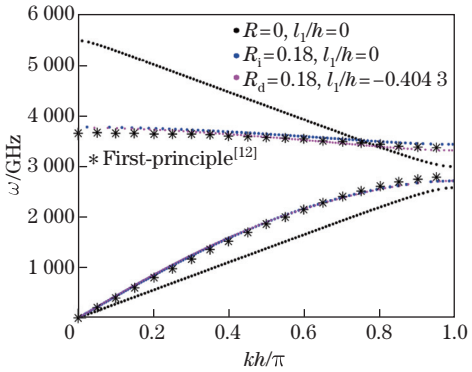

Fig. 4 First two bands of the vertically incident SH waves in the HfO_2-ZrO_2 periodic layered nanostructure (color online)

density in the periodic layered nanostructure. A general relation is presented below for possible future design use.

Figure 5 predicts the important relation between the interface mass density and the internal characteristic length when $R\,(=R_{\rm i}=R_{\rm d})\leqslant 0.3$ for the vertical SH waves. Along this special curve, the dispersion curves obtained by the nonlocal differential model with the interface mass density are the same as those based on the nonlocal integral model in the low frequency region ($\Omega<2$). It is observed from Fig. 5 that, for the given R and within the low frequency range, the dispersion curves based on the nonlocal differential model can be tuned to be exactly the same as those based on the nonlocal integral model, thus providing us with a possible channel to inverting the interface mass density of the given periodic layered nanostructure.

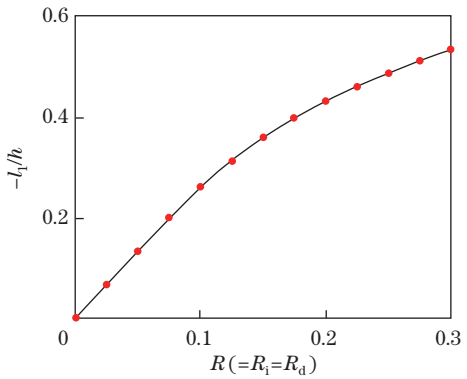

Fig. 5 A general theoretical relation between the dimensionless internal characteristic length and the dimensionless (negative) interface mass density (color online)

Before we switch to the obliquely incident SH waves case, we show in Fig. 6 the band structures of the same periodic layered nanostructure when $R\,(=R_{\rm i}=R_{\rm d})=0.15$ and when frequency is relatively high. While the band gaps are almost the same before the cut-off frequency based on the nonlocal integral model, there are two extra bands after the last dense zone when the nonlocal differential model combined with the interface effect is used. This phenomenon happens only when the internal characteristic length R is relatively large.

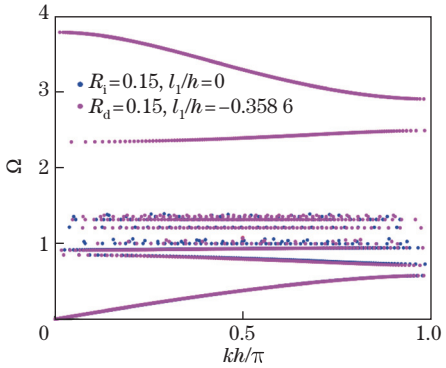

Fig. 6 Dispersion curves for SH waves vertically incident to the HfO_2-ZrO_2 periodic layered nanostructure (color online)

4.2 Oblique incidence

Now, we investigate the SH waves when the incident angle is 30° to the HfO_2-ZrO_2 periodic layered nanostructure. The dispersion curves are shown in Fig. 7(a) for the nonlocal model

without the interface effect ($l_1/h = 0$), in Fig. 7(b) for the local case ($R = 0$) with the interface effect, and in Fig. 7(c) for combined effects. Similar to the vertical incidence case, we see that the band structures described by the nonlocal integral model and the nonlocal differential model with the interface effect could be tuned to be the same by properly choosing the interface parameters. While the interface density can be characterized by the vertically incident waves (see Figs. 3 and 4), the interface shear modulus can be predicted by matching the dispersion curves of the obliquely incident SH waves. This is discussed further below.

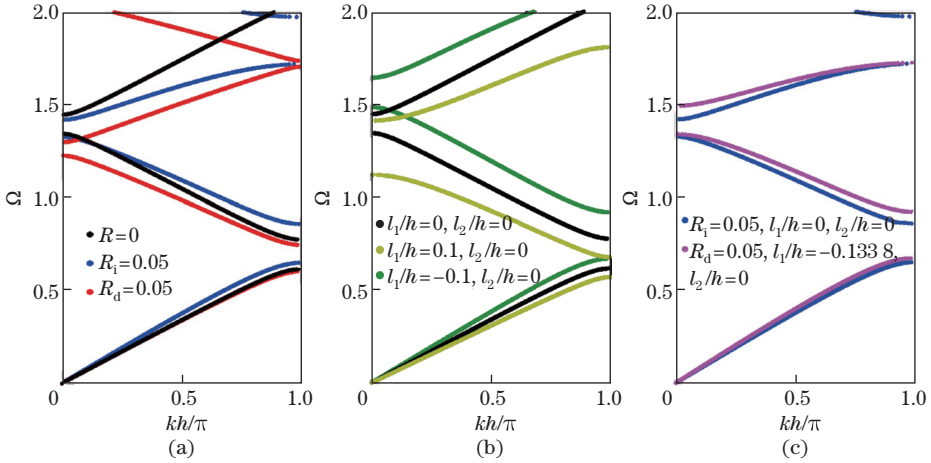

Fig. 7 Dispersion curves for SH waves obliquely incident to the HfO_2-ZrO_2 periodic layered nanostructure (at an angle of 30°), (a) the nonlocal model without the interface effect ($l_1/h = 0$, $l_2/h = 0$), (b) the local model ($R = 0$) with the interface effect, and (c) the model with combined effects (color online)

Figure 8 shows the dispersion curves of the obliquely incident SH waves (at an incident angle of 30°) when $R(= R_i = R_d) = 0.05$, 0.1, and 0.15. It is observed that, the band structures obtained by the nonlocal integral model are almost the same as those obtained by the nonlocal differential model combined with the interface effect. This feature again indicates that there exist some intrinsic relations between the internal characteristic length and the interface parameters. Furthermore, by comparing Fig. 8(b) with Fig. 3(b), we can easily see

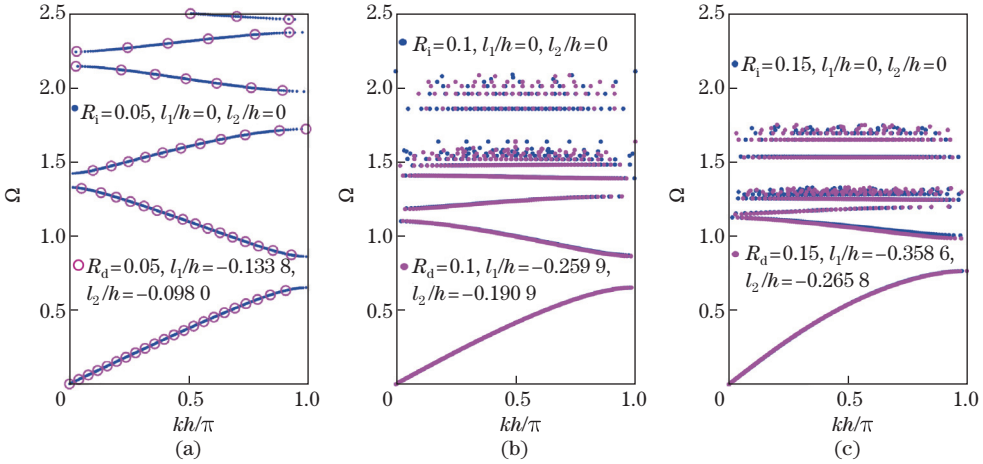

Fig. 8 Dispersion curves of the SH waves obliquely incident to the HfO_2-ZrO_2 periodic layered nanostructure at an angle of 30° (color online)

that the cut-off frequency of the obliquely incident SH waves is roughly the same as that of the vertically incident SH waves.

The relation between the internal characteristic length and the interface shear modulus is presented in Fig. 9. When $R = R_{\mathrm{i}} = R_{\mathrm{d}}$, the dispersion curves obtained by the nonlocal differential model combined with the interface effect can be tuned to be the same as those based on the nonlocal integral model at the low frequency region. However, different from the vertically incident waves, for the case of oblique incidence, both the interface mass density and the interface shear modulus need to be tuned. Since the interface mass density can be tuned from the vertically incident dispersion curves, here for the obliquely incident waves, we only need to tune the interface shear modulus. As such, combining both the vertically and obliquely incident SH waves, one could invert all the interface parameters (both the interface mass density and the interface shear modulus) for the given internal characteristic length.

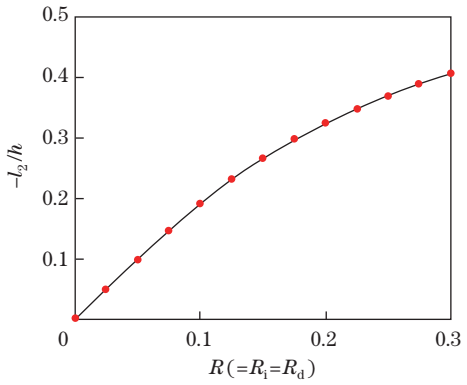

Fig. 9 A general theoretical relation between the interface shear modulus and the internal characteristic length for the SH waves propagating obliquely incident to the HfO_2-ZrO_2 periodic layered nanostructure, where the interface mass density used is the one tuned from the vertically incident SH waves in Fig. 5 (color online)

Furthermore, we point out that even though both the nonlocal integral model and the nonlocal differential model combined with the interface effect can be used to predict the band nanostructure, both approaches have their own advantages and disadvantages. For example, the nonlocal integral model has only one scale parameter, but it contains a couple of integrated items, which could be difficult to calculate for problems involving a high-dimensional and complex geometric shape. On the other hand, the nonlocal differential model combined with the interface effect has a relatively simple mathematical expression, but it involves more parameters which need to be determined.

5 Conclusions

Based on the nonlocal elastic continuum theory and the interface theory, the propagation properties of SH waves in periodic layered nanocomposites are studied by using the transfer matrix method and the Block theory. The differences and relations among the nonlocal integral model, the nonlocal differential model, and the latter model with the interface effect are studied via their band structures. Numerical examples show further the effects of the internal characteristic length and the interface parameters on the band structures. From our numerical results, the following conclusions can be drawn.

(i) By choosing appropriate interface parameters, the dispersion relation of the SH waves predicted by the nonlocal integral model can be tuned in good agreement with that obtained by

the nonlocal differential model combined with the interface effect. This feature holds for both vertically and obliquely incident waves to the periodic layered nanostructure at a low frequency.

(ii) Interface parameters have no effect on the cut-off frequency when considering the nonlocal theory. In other words, the cut-off frequency will be the same when the internal characteristic length is small, no matter whether the nonlocal integral or differential model is used.

(iii) The cut-off frequency of the obliquely incident waves is almost the same as that of the vertically incident waves.

(iv) By matching the SH waves band structures obtained based on the two different nonlocal models, we could invert the interface mass density when the wave is vertically incident and invert the interface shear modulus when the waves is obliquely incident.

References

[1] SIGALAS, M. M. and ECONOMOU, E. N. Elastic and acoustic wave band structure. *Journal of Sound and Vibration*, **158**, 377–382 (1992)

[2] KUSHWAHA, M. S., HALEVI, P., DOBRZYNSKI, L., and DJAFARI-ROUHANI, B. Acoustic band structure of periodic elastic composites. *Physical Review Letters*, **71**(13), 2022–2025 (1993)

[3] GUO, X., LIU, H., ZHANG, K., and DUAN, H. L. Dispersion relations of elastic waves in two-dimensional tessellated piezoelectric phononic crystals. *Applied Mathematical Modelling*, **56**, 65–82 (2018)

[4] ZHENG, H., ZHANG, C., and YANG, Z. A local radial basis function collocation method for band structure computation of 3D phononic crystals. *Applied Mathematical Modelling*, **77**, 1954–1964 (2020)

[5] WU, L. Y., WU, M. L., and CHEN, L. W. The narrow pass band filter of tunable 1D phononic crystals with a dielectric elastomer layer. *Smart Materials and Structures*, **18**(1), 015011 (2009)

[6] RONDA, S. and MONTERO DE ESPINOSA, F. Design of piezoelectric piston-like piezoelectric transducers based on a phononic crystal. *Advances in Applied Ceramics*, **117**(3), 177–181 (2017)

[7] CERVERA, F., SANCHIS, L., SÁNCHEZ-PÉREZ, J. V., MARTÍNEZ-SALA, R., RUBIO, C., MESEGUER, F., LÓPEZ, C., CABALLERO, D., and SÁNCHEZ-DEHESA, J. Refractive acoustic devices for airborne sound. *Physical Review Letters*, **88**(2), 023902 (2002)

[8] BENCHABANE, S., KHELIF, A., CHOUJAA, A., DJAFARI-ROUHANI, B., and LAUDE, V. Interaction of waveguide and localized modes in a phononic crystal. *Europhysics Letters*, **71**(4), 570–575 (2005)

[9] WONG, E. W., SHEEHAN, P. E., and LIEBER, C. M. Nanobeam mechanics: elasticity, strength, and toughness of nanorods and nanotubes. *Science*, **277**(5334), 1971–1975 (1997)

[10] WANG, Z. L. and SONG, J. H. Piezoelectric nanogenerators based on zinc oxide nanowire arrays. *Science*, **312**(5771), 242–246 (2006)

[11] EBRAHIMI, F. and BARATI, M. R. Dynamic modeling of preloaded size-dependent nano-crystalline nano-structures. *Applied Mathematical and Mechanics* (*English Edition*), **38**(12), 1753–1772 (2017) https://doi.org/10.1007/s10483-017-2291-8

[12] RAMPRASAD, R. and SHI, N. Scalability of phononic crystal heterostructures. *Applied Physics Letters*, **87**(11), 101101 (2005)

[13] FARAJPOUR, A., GHAYESH, M. H., and FAROKHI, H. A review on the mechanics of nanostructures. *International Journal of Engineering Science*, **133**, 231–263 (2018)

[14] TOUPIN, R. A. Elastic materials with couple-stresses. *Archive for Rational Mechanics and Analysis*, **11**(1), 385–414 (1962)

[15] MINDLIN, R. D. and TIERSTEN, H. F. Effects of couple-stresses in linear elasticity. *Archive for Rational Mechanics and Analysis*, **11**(1), 415–448 (1962)

[16] ERINGEN, A. C. *Theory of Micropolar Elasticity*, Springer, New York, 101–248 (1999)

[17] MINDLIN, R. D. Second gradient of strain and surface-tension in linear elasticity. *International Journal of Solids and Structures*, **1**(4), 417–438 (1965)

[18] ERINGEN, A. C. and EDELEN, D. G. B. On nonlocal elasticity. *International Journal of Engineering Science*, **10**, 233–248 (1972)

[19] ERINGEN, A. C. On differential equations of nonlocal elasticity and solutions of screw dislocation and surface waves. *Journal of Applied Physics*, **54**(9), 4703–4710 (1983)

[20] LIM, C. W., ZHANG, G., and REDDY, J. N. A higher-order nonlocal elasticity and strain gradient theory and its applications in wave propagation. *Journal of the Mechanics and Physics of Solids*, **78**, 298–313 (2015)

[21] LU, L., GUO, X. M., and ZHAO, J. Z. Size-dependent vibration analysis of nanobeams based on the nonlocal strain gradient theory. *International Journal of Engineering Science*, **116**, 12–24 (2017)

[22] GURTIN, M. E. and MURDOCH, A. I. A continuum theory of elastic material surfaces. *Archive for Rational Mechanics and Analysis*, **57**(4), 291–323 (1975)

[23] GURTIN, M. E. and MURDOCH, A. I. Surface stress in solids. *International Journal of Solids and Structures*, **14**(6), 431–440 (1978)

[24] CHEN, A. L. and WANG, Y. S. Size-effect on band structures of nanoscale phononic crystals. *Physica E*: *Low-dimensional Systems and Nanostructures*, **44**(1), 317–321 (2011)

[25] CHEN, A. L., WANG, Y. S., KE, L. L., GUO, Y. F., and WANG, Z. D. Wave propagation in nanoscaled periodic layered structures. *Journal of Computational and Theoretical Nanoscience*, **10**(10), 2427–2437 (2013)

[26] CHEN, J. Y., GUO, J. H., and PAN, E. Wave propagation in magneto-electro-elastic multilayered plates with nonlocal effect. *Journal of Sound and Vibration*, **400**, 550–563 (2017)

[27] ZHANG, L. L., LIU, J. X., FANG, X. Q., and NIE, G. Q. Effects of surface piezoelectricity and nonlocal scale on wave propagation in piezoelectric nanoplates. *European Journal of Mechanics-A/Solids*, **46**, 22–29 (2014)

[28] WU, B., ZHANG, C. L., CHEN, W. Q., and ZHANG, C. Surface effects on anti-plane shear waves propagating in magneto-electro-elastic nanoplates. *Smart Materials and Structures*, **24**(9), 095017 (2015)

[29] JIA, F., ZHANG, Z. C., ZHANG, H. B., FENG, X. Q., and GU, B. Shear horizontal wave dispersion in nanolayers with surface effects and determination of surface elastic constants. *Thin Solid Films*, **645**, 134–138 (2018)

[30] ZHU, F., PAN, E., QIAN, Z. H., and WANG, Y. Dispersion curves, mode shapes, stresses and energies of SH and Lamb waves in layered elastic nanoplates with surface/interface effect. *International Journal of Engineering Science*, **142**, 170–184 (2019)

[31] ERINGEN, A. C. *Nonlocal Continuum Field Theories*, Springer, New York (2002)

[32] SEITZ, F., TURNBULL, D., and EHRENREICH, H. *Solid State Physics*, Academic Press, New York (1968)

[33] MINDLIN, R. E. *Progress in Applied Mechanics* (*the Prager Anniversary Volume*), Macmillan, New York (1963)

[34] TIERSTEN, H. F. Elastic surface waves guided by thin films. *Journal of Applied Physics*, **40**(2), 770–789 (1969)

[35] SHENOY, V. B. Atomistic calculations of elastic properties of metallic FCC crystal surfaces. *Physical Review B*, **71**, 094104 (2005)

[36] HE, J. and ZHAO, J. L. Finite element simulations of surface effect on Rayleigh waves. *AIP Advances*, **8**, 035006 (2018)

Appendix A

The matrices $\boldsymbol{M}$ and $\boldsymbol{N}$ in Eq. (16) are given by

$$\boldsymbol{M} = \begin{pmatrix} 1 & 1 \\ \dfrac{-\mathrm{i}\rho c_{\mathrm{sh}}^2 q}{1+R^2q^2+R^2\beta^2} & \dfrac{\mathrm{i}\rho c_{\mathrm{sh}}^2 q}{1+R^2q^2+R^2\beta^2} \end{pmatrix}, \tag{A1}$$

$$\boldsymbol{N} = \begin{pmatrix} \mathrm{e}^{-\mathrm{i}q\xi} & \mathrm{e}^{\mathrm{i}q\xi} \\ \dfrac{-\mathrm{i}\rho c_{\mathrm{sh}}^2 q\mathrm{e}^{-\mathrm{i}q\xi}}{1+R^2q^2+R^2\beta^2} & \dfrac{\mathrm{i}\rho c_{\mathrm{sh}}^2 q\mathrm{e}^{\mathrm{i}q\xi}}{1+R^2q^2+R^2\beta^2} \end{pmatrix} \tag{A2}$$

for the nonlocal differential model, and

$$\boldsymbol{M} = \begin{pmatrix} 1 & 1 \\ \dfrac{\mathrm{i}\rho c_{\mathrm{sh}}^2 q(\mathrm{e}^{-\mathrm{i}q\overline{h}}\mathrm{e}^{-\overline{h}/R}-1)}{2(1+\mathrm{i}Rq)} & \dfrac{-\mathrm{i}\rho c_{\mathrm{sh}}^2 q(\mathrm{e}^{\mathrm{i}q\overline{h}}\mathrm{e}^{-\overline{h}/R}-1)}{2(1-\mathrm{i}Rq)} \end{pmatrix}, \tag{A3}$$

$$\boldsymbol{N} = \begin{pmatrix} \mathrm{e}^{-\mathrm{i}q\xi} & \mathrm{e}^{\mathrm{i}q\xi} \\ \dfrac{-\mathrm{i}\rho c_{\mathrm{sh}}^2 q(\mathrm{e}^{-\mathrm{i}q\overline{h}}-\mathrm{e}^{-\overline{h}/R})}{2(1-\mathrm{i}Rq)} & \dfrac{\mathrm{i}\rho c_{\mathrm{sh}}^2 q(\mathrm{e}^{\mathrm{i}q\overline{h}}-\mathrm{e}^{-\overline{h}/R})}{2(1+\mathrm{i}Rq)} \end{pmatrix} \tag{A4}$$

for the nonlocal integral model.

The matrix $\boldsymbol{P}$ in Eq. (19) is given by

$$\boldsymbol{P} = \begin{pmatrix} 0 & 0 \\ -\rho_{\mathrm{s}}\omega^2+\mu_{\mathrm{s}}\beta^2/m_{\mathrm{s}} & -\rho_{\mathrm{s}}\omega^2+\mu_{\mathrm{s}}\beta^2/m_{\mathrm{s}} \end{pmatrix}, \tag{A5}$$

where $m_{\mathrm{s}}=1$ for the nonlocal integral model, and $m_{\mathrm{s}}=1+R^2q^2+R^2\beta^2$ for the nonlocal differential model.